

## VERIFICATION TESTS OF THE DYNAMIC BEHAVIOR OF THE NOVEL FRICTION-BASED ROTATIONAL DAMPER USING SHAKING TABLE

A. Toyooka<sup>1</sup>, T. Himeno<sup>2</sup>, Y. Hishijima<sup>3</sup>, H. Iemura<sup>4</sup> and I. Mualla<sup>5</sup>

<sup>1</sup> Dept. of Urban Management, Kyoto Univ., Japan

<sup>2</sup> Professional Eng., Kawaguchi Metal Industry, Japan

<sup>3</sup> Head of Tech. Dept., Kawaguchi Metal Industry, Japan

<sup>4</sup> Professor Emeritus, Kyoto Univ., Japan

<sup>5</sup> Chief Technical Officer of DAMPTECH, DTU, Denmark

Email: toyooka@catfish.kuciv.kyoto-u.ac.jp, himeno@kawakinkk.co.jp, hishijima@kawakinkk.co.jp,  
iemura@catfish.kuciv.kyoto-u.ac.jp, ihm@damptech.com

### ABSTRACT :

A friction damper is regarded as one of the most effective structural control devices in view of regulating the inertia force induced from the upper structures and effective energy dissipation. Despite a large number of friction dampers or bearings have been used for civil and architectural structures, those devices generally require large deformation and stable vertical load induced on the device in order to attain a desirable control performance.

In order to overcome such difficulties, a new friction-based damper was developed. The new damper has several steel arms that are linked each other by a bolt in order for them to rotate freely, and carefully manufactured disk friction materials are embedded in that link. By connecting these arms to the upper and lower structures, horizontal deformation of the structure is converted into the rotational motion of the link and disk. The damper requires significantly less space for installation compared to the traditional friction dampers in order to attain the large friction energy dissipation. Moreover, the friction force is easily controlled by a torque of the fastening bolt, independent from the vertical load of the upper structure.

In this research, dynamic performance of the proposed damper was studied through a large-scale shaking table tests on which the girder and bearings were mounted. It was confirmed through periodical loading tests that the damper generated the stable friction force regardless of the loading frequency. It was also found that the damper successfully introduced the supplemental damping to the structure under earthquake motions.

**KEYWORDS:** Bridge Damper, Passive Control, Experimental Tests, Friction Damper, Bridges Retrofitting

### 1. INTRODUCTION

Due to its proven efficiency, the concept of seismic protection based on supplemental damping is gaining momentum within the engineering community worldwide. Friction dampers are often employed in passive response control systems because of their high-energy dissipation potential at relatively low cost and they are easy to install and maintain. Most of the bridges around the world are having dampers. Dampers, they become a very essential and important part of the bridges in order to protect the bridges from heavy dynamic vibration caused by seismic, wind and traffic vibration, and also as bridge retainers.

There exists a variety of devices capable of absorbing seismic energy. The research reported herein is focused in particular on the performance of a new Friction Damper Device (FDD) developed by Mualla (Mualla, 2000) for frame structures. The complete damping system includes FDDs supported by secondary structure. A comprehensive testing of different models and sizes were carried out at the Technical University of Denmark (DTU). A special high tech friction material was heavily evaluated and tested. This friction material performed very well in all aspects and seems very promising one.

However, further research was needed to verify the performance of the damping system in bridges and elevated highways in full-scale application under seismic ground shaking. This paper presents results of a co-operative international research program with Kawaguchi Metal Industry, Kyoto University and DAMPTECH for experimental investigation of the FDD using for bridges. In this research, the prototype damper designed for civil engineering structures was developed and tested using the large-scale shaking table facility. The girder consisting of the counterweight, bearings and prototypes of the proposed damper were mounted on the shake table and excited by sinusoidal waves as well as strong earthquakes. Through the series of tests, the dynamic relation between friction force and displacement, its dependency on loading frequency and the amount of the supplemental damping introduced to the structure were mainly discussed.

## 2. BASIC CONCEPT OF THE PROPOSED NEW DAMPER

The schematic as well as basic principle of the proposed damper are shown in Figures 1 and 2, respectively. The new damper has several steel arms one ends of which are linked each other by a bolt in order for them to rotate freely, and carefully manufactured disk friction materials are embedded in that link. By connecting both ends of these arms to the upper and lower structures, horizontal deformation of the girder is converted into the rotational motion of the link and disk. To be more precise, the horizontal force  $F$  in Figure 2 balances with the friction moment  $M$ , depending on the moment arm length  $L$ .

One of the key features of the proposed damper is its easiness of installation and maintenance. It requires significantly less space for installation compared to the traditional friction dampers in order to attain the large friction energy dissipation. In addition, the axial force that significantly affects the performance of the friction type device is easily controlled by a torque of the fastening bolt, independent from the vertical load of the upper structure. That is to say, the damper can be installed in a short time without a need to high tech equipments or highly trained qualified staff. From the viewpoint of the long-term durability, the damper has a very stable performance over many cycles because of the special friction material. The damper shows a reliable performance over multiple earthquakes. Also, the damper is easily maintained if necessary and if required, can be easily replaced after severe earthquakes.

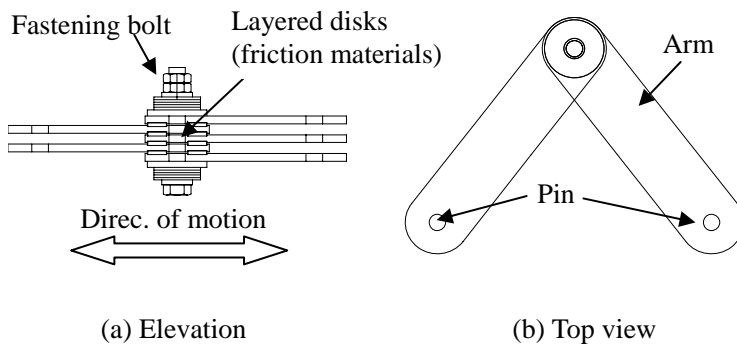


Figure 1 Schematic of the proposed damper

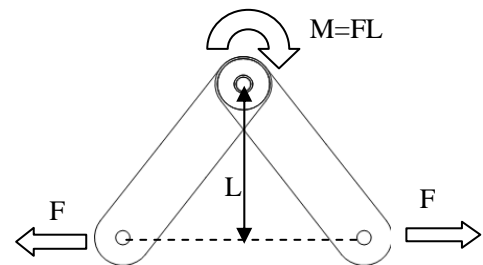


Figure 2 Basic mechanism of the damper

## 3. SHAKING TABLE TEST

### 3.1 Test setup

The prototype of the proposed damper was designed on the basis of the concepts mentioned above, and its dynamic behavior was assessed by using the large-scale shaking table facility in Disaster Prevention Research Institute of Kyoto University. The shake table has a capability to drive the table (5.0 m×3.0 m) up to 1.0 G in acceleration and 150 kine in velocity with maximum specimen weight of 150 kN. The maximum strokes are 300 mm in longitudinal, 250 mm in transverse, and 200 mm in up-down directions.

As shown in Photo 1, large-scale model of an isolated girder was assembled on the shake table. The model of the girder was a steel-made slab (W4150 mm×D2650 mm×H400 mm), the weight of which was approximately 100 kN. For supporting the girder, two different setups were prepared as shown in Figure 3. The girder was supported by four natural rubber bearings (Setup 1), or two natural rubber bearings plus four slide bearings (Setup 2). The setup 1 was prepared for both sinusoidal and earthquake excitation tests, and setup 2 for sinusoidal loading tests. The specifications of the rubber bearing for setups 1 and 2 are shown in Table 3.1. The equivalent stiffness and corresponding damping ratio in the table were obtained by preliminary cyclic loading tests, in which maximum strain was 136 %, loading frequency was 0.05 Hz and number of repetitions was 10. For slide bearings in setup 2, 290-mm-square stainless-steel plates and polyamide portion were combined, the friction coefficient of which was approximately 0.05. The natural periods of these systems were 0.42 sec and 0.60 sec, respectively. As seen in Figure 3 and Photo 2, four damper specimens were then prepared and placed at the every edges of the girder.

Table 3.1 Specifications of the rubber bearings

Shear modulus	0.8 N/mm <sup>2</sup>
Rubber thickness per layer	10 mm
Number of layers	7
Equivalent stiffness (strain=136%)	0.553 kN/mm
Equivalent damping ratio (strain=136%)	7.97 %

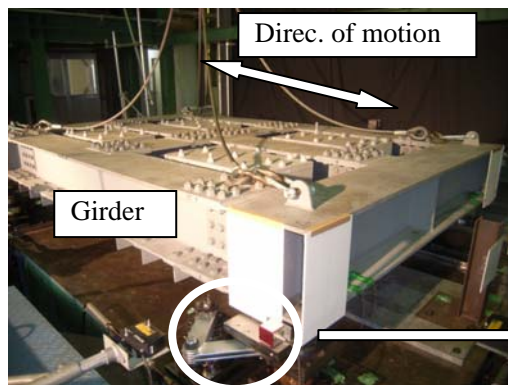


Photo 1. Test setup

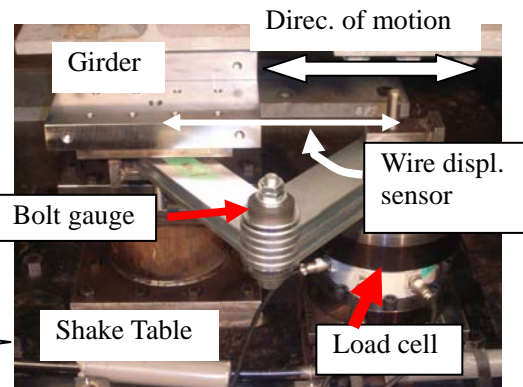
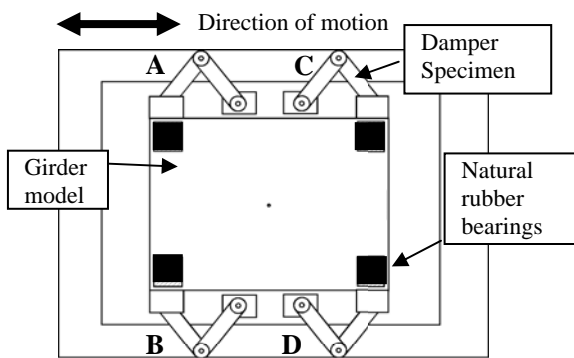
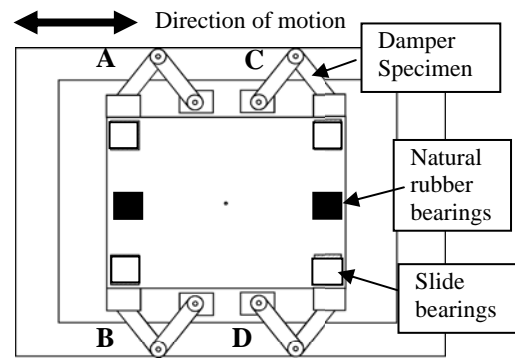


Photo 2. Damper specimen and sensors

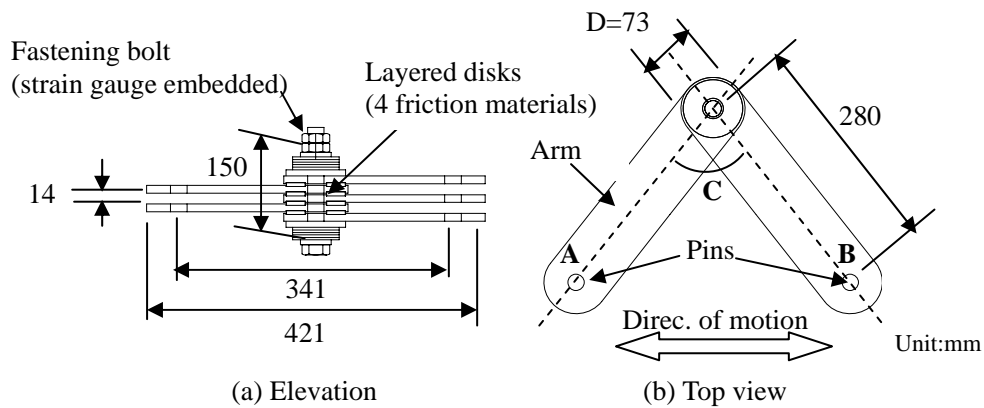


(a) Setup 1 (Natural period = 0.42 sec)



(b) Setup 2 (Natural period = 0.60 sec)

Figure 3 Schematics of the test setups



(a) Elevation

(b) Top view

Figure 4 Specification of the damper specimen

### 3.2 Data acquisition

Several accelerometers and laser displacement transducers were embedded on the girder and the shake table in order to comprehend the motion of the girder. For the damper specimens, three different types of sensors were installed: wire displacement sensor, load transducer and bolt gauge. The wire displacement sensors were used to measure the relative displacement between two links attached to the girder and the shake table. The load transducers were attached to the all dampers to directly measure the damper's horizontal forces, regardless of the characteristics of the behavior of the total test setup.

The bolt gauge, embedding a strain gauge in the fastening bolt, was prepared to comprehend the initial torque as well as the fluctuation of the axial force during the test.

### 3.3 Specification of the damper specimen

As shown in Figure 3, total four dampers were prepared and installed to the test system. Figure 4 shows the specification of the damper specimen for the test. Both ends of the arm, A and B in the figure, were attached to the girder model and the load transducer mounted on the shake table using pins (see Photo 2). Prior to the every loading test, the fastening bolt in Figure 4 was fastened so that the initial axial force was approximately 15 kN. In addition, initial angle of the damper, C in the figure, was also measured to estimate the time history of the rotation angle by means of the arm length and relative displacement between A and B in the figure.

### 3.4 Input motions

The shaking table was driven in longitudinal direction by both sinusoidal and earthquake motions. The number of sinusoidal motions with various amplitude and frequency were prepared to clarify the dependencies of the damper's dynamic behavior on stroke and stroke velocity of excitation.

As for earthquake excitations, two different types of the acceleration waveforms based on strong motion records were used. The recorded earthquake at Onnetto bridge during the 1994 Hokkaido-Toho-Oki earthquake (Onneto Br. wave) was selected for assuming inter-plate earthquake, a duration time of which is relatively long. On the contrary, the North-South component of the JR Takatori station record during the 1995 Hyogoken-Nambu earthquake (JR Takatori wave) was also chosen as very-rare inland intense earthquake. The waveforms and corresponding linear displacement response spectra at damping of 5% are shown in Figures 5 and 6, respectively. The time steps of these waves were scaled by means of a law of similarity so that the apparent natural periods of the test setup 1 were approximately 0.85 sec and 1.06 sec, respectively. This conversion intended to excite the damper with a large displacement, namely, no corresponding real structures were assumed in the series of tests.

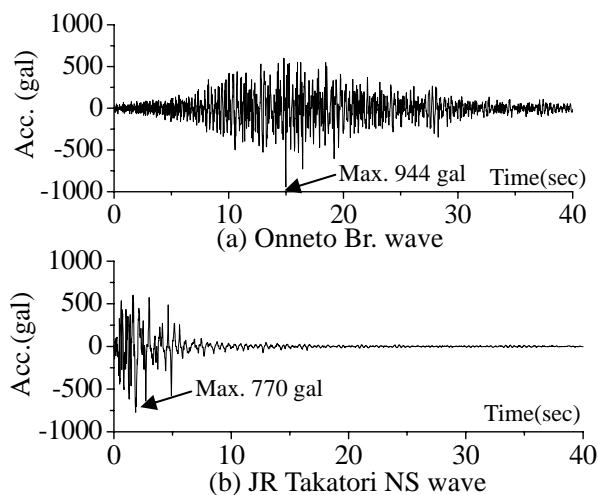


Figure 5 Input earthquake motions

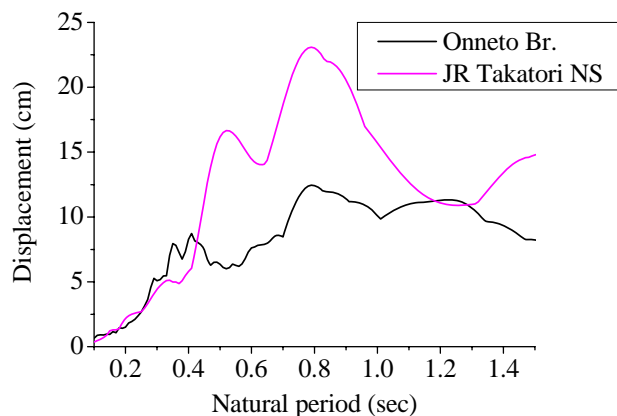


Figure 6 Linear displacement response spectra of input motions at damping of 5%

## 4. TEST RESULTS AND DISCUSSIONS

### 4.1 Sinusoidal loading tests

Figure 7 shows the representative relations between total damper forces and displacements under sinusoidal motions; 1) Test setup 1 was subjected to the frequency of 1.7 Hz and maximum acceleration of 300 gal (Figure 7(a)) and 2) Test setup 2 excited by a motion of 2.8Hz, 300 gal (Figure 7(b)). The horizontal forces in the figure were obtained by the sum of four dampers. Since the frequencies of input motions were adjacent to the natural frequencies of test systems in both cases, dampers were supposed to the various levels of excitations as the displacement was gradually approaching to the steady-state response. As seen in the figure, dampers generated stable friction forces under periodical motion, independent of the displacement. It consequently follows that the proposed damper holds the same advantage as ordinal friction devices over other types of structural control devices that regulates the interactive force between upper and lower structures up to its friction level. It should be noted that the proposed device attained such a performance without requiring large amount of sliding area.

As for behavior of each damper, momentum force versus relative rotation angle of arms is depicted in Figure 8. It is observed from the figure that all the dampers worked almost equally from the standpoint of the momentum forces and hysteretic behaviors.

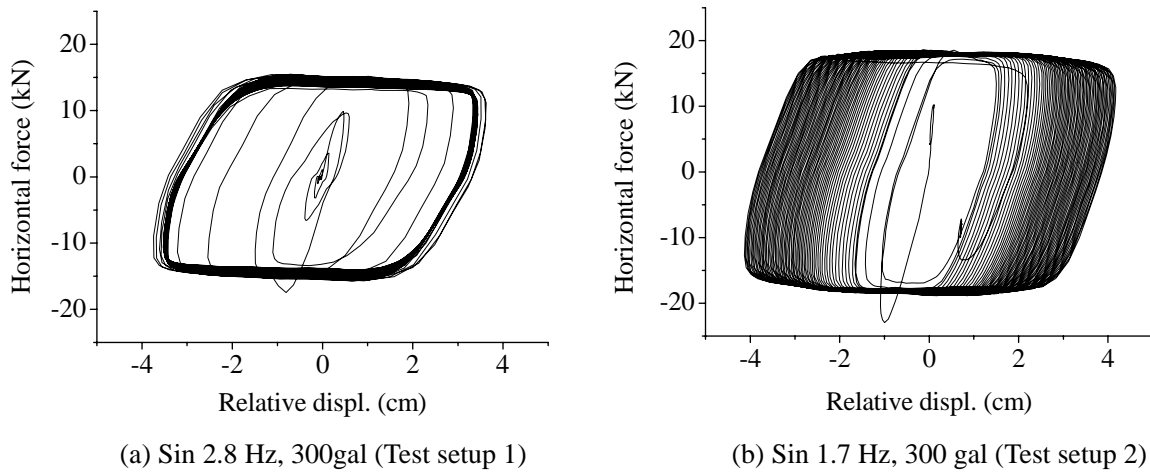


Figure 7 Damper forces v.s. relative displacements relations

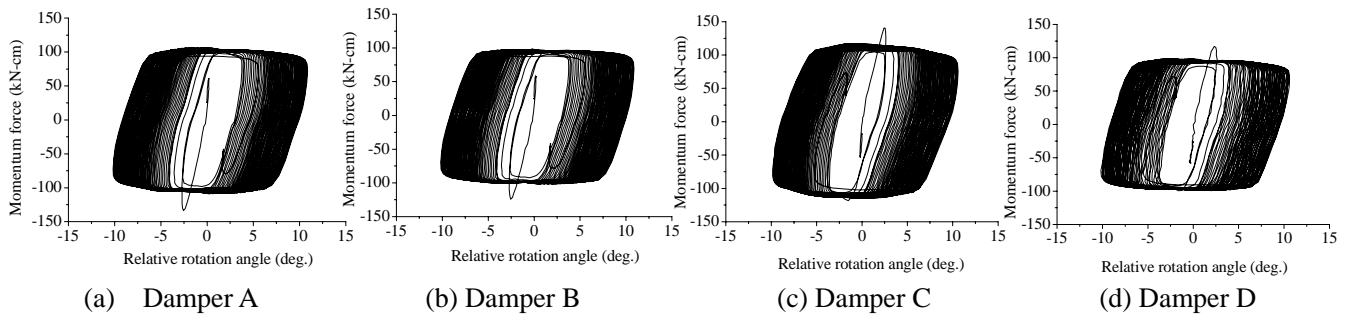


Figure 8 Moment v.s. relative rotation angle relations of all dampers (Sin 1.7 Hz, 300 gal, Test setup2)

One of the significant and interesting features of the damper is its dependency on loading frequency. Several cyclic excitation tests were carried out in order to examine the fluctuation of the moment under various loading speeds. Table 4.1 shows the list of frequency and maximum acceleration for the test setups 1 and 2. The loading frequencies were selected in order to attain a certain amount of damper stroke and to cover dominant natural periods of the common civil engineering structures. In each test case, a mode of the absolute momentum force over time history is selected as representative value of the damper’s total hysteresis. The obtained momentum force was then divided by the initial axial force of the fastening bolt to eliminate the dependency of the stress induced on the friction material. Figure 9 illustrates the relation between the normalized moments and corresponding loading frequencies, correlation coefficient of that was -0.28. It can be observed that the momentum force was not significantly affected by the loading frequency. In other words, the proposed damper has a capability to attain stable energy dissipation under wide-range of loading frequencies.

Table 4.1 Test cases for sinusoidal loadings

Test setup 1		Test setup 2	
Freq.(Hz)	Acc (gal)	Freq.(Hz)	Acc (gal)
2.0	400, 450	1.0	300
2.4	300	1.5	300
2.5	300	2.3	250
2.8	300	2.5	250
2.9	300	2.6	250
3.0	300	2.7	250
3.3	300	3.0	250
3.5	300		

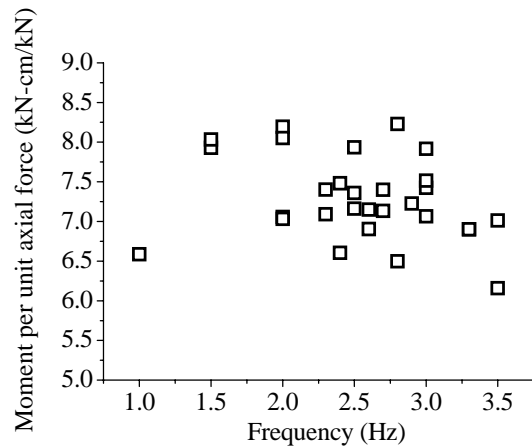


Figure 9 Excitation frequency versus moment (per unit axial bolt force) relation

4.2 Earthquake loading tests

On the basis of the sinusoidal loading tests, earthquake excitation tests were conducted using the test setup 1 to verify the damper’s capability of energy dissipation under non-periodical excitation.

Figure 10 shows hysteretic loops of four dampers’ total horizontal force, corresponding friction moment and relative displacement under Onneto Br. motion. The same relations in case of JR Takatori excitation are depicted in Figure 11. It is observed from the figures that the damper behaved as an elasto-plastic material, the horizontal forces of which were successfully saturated at a friction force of approximately 25 kN.

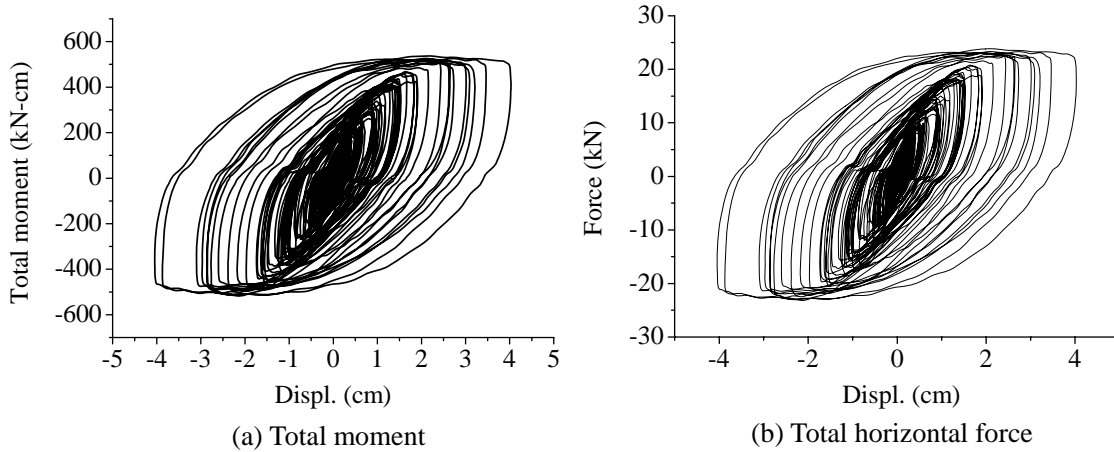


Figure 10 Damper total moment/force v.s. relative displacement (Onneto Br. input)

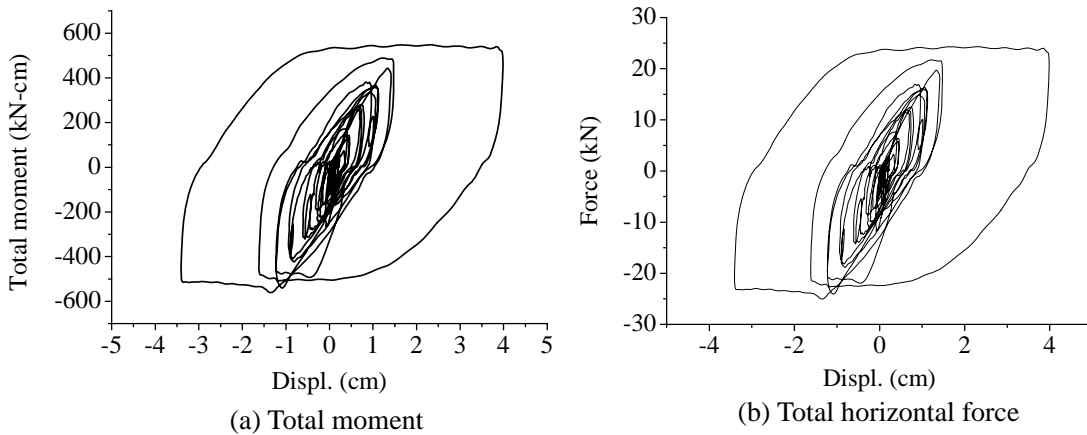


Figure 11 Damper total moment/force v.s. relative displacement (JR Takatori NS input)

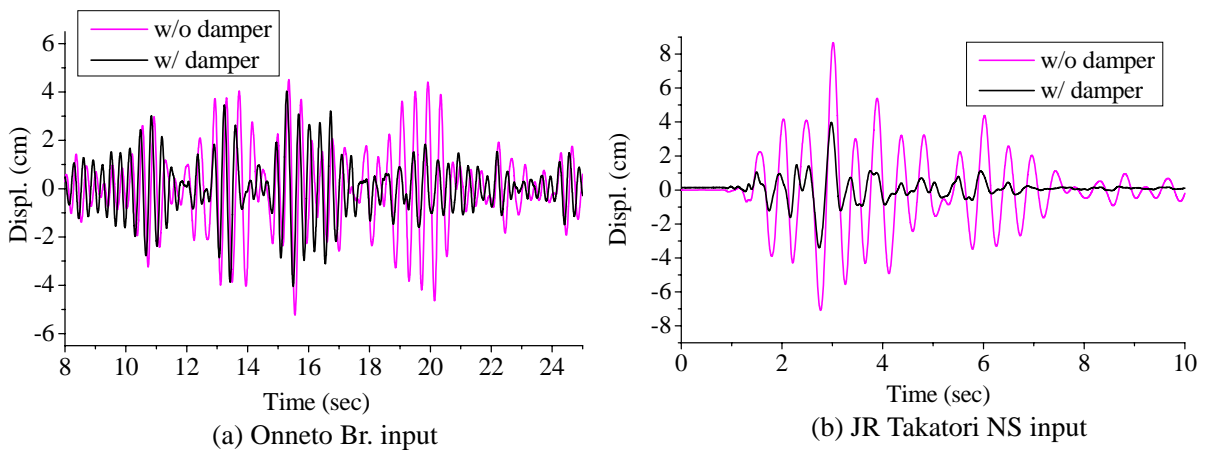


Figure 12 Relative displacements (shake table – girder) with and without dampers

As for the vibration reduction performance, Figure 12 illustrates the girder's relative displacements from the shake table under earthquake motions as a comparison with and without dampers. The responses without dampers were calculated by numerical simulations incorporating the specifications of the girder and bearings shown in Table 3.1, since those were not obtained experimentally due to the stroke limitations of the rubber bearings. It is found from these time histories that the maximum responses of the displacement were reduced from 5.23 cm to 4.04 cm (reduced by 22.8 %) in case of Onneto Br. motion, and 8.68 cm to 3.98 cm (reduced by 54.2 %) in JR Takatori input. This difference in response reduction effect partly arises from the amount of the damping induced to the test system, depending on the frequency characters of the input motion.

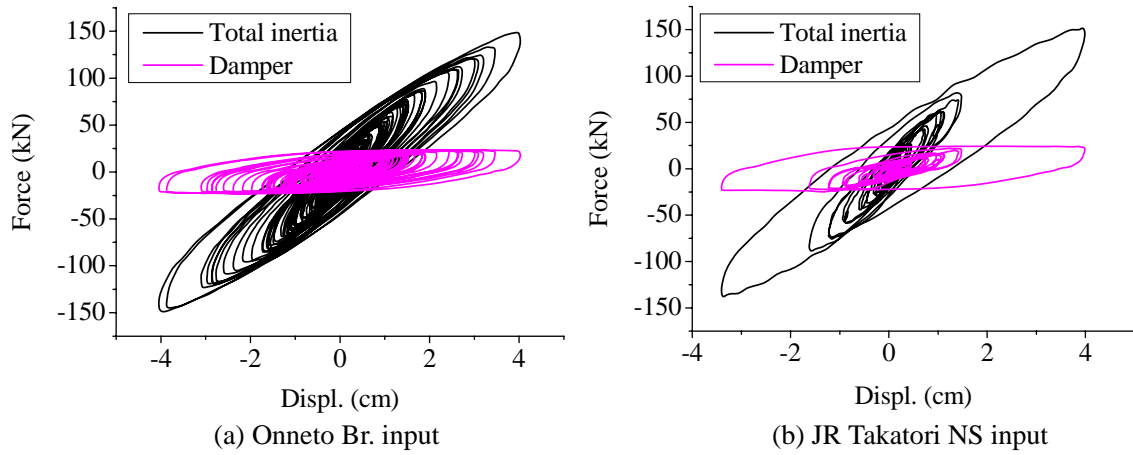


Figure 13 Inertial and damping forces versus displacement relations

In order to assess the energy dissipation performance of the damper quantitatively, the amount of the supplemental damping induced by the damper was estimated by a following procedures. Figure 13 shows inertia force versus displacement relations of both earthquake motions. The hysteretic loops of dampers are also depicted in the same figures. It is clearly observed from the figure that the damper's forces in both cases were restrained at its friction force, whereas the total inertias increased in accordance with the displacement. The residual force, arises from the structural elements such as rubber supports and other damping elements included in the test system, was obtained by subtracting the damper's force from the inertia. Suppose the hysteretic behaviors with regard to the inertial as well as the residual forces are expressed by a linear combination of displacement and velocity, say,

$$I(t) = kx + cv, \quad F_s(t) = k_s x + c_s v. \quad (4.1)$$

Where,  $I$  and  $F_s$  are forces due to inertia and structural elements,  $k$ ,  $c$  are equivalent stiffness and damping coefficients of the total test system,  $k_s$ ,  $c_s$  are those for the residual force, and  $x$ ,  $v$  are experimentally obtained displacement and velocity. These stiffness and viscous coefficient were identified by employing a nonlinear least square method, minimizing the following evaluation functions.

$$E_e = \int_0^T |(I_e(t) - I(t)) x(t)|^2 dt, \quad E_s = \int_0^T |(F_{se}(t) - F_s(t)) x(t)|^2 dt \quad (4.2)$$

In these functions,  $I_e$  and  $F_{se}$  express experimentally obtained inertial and residual forces, and  $T$  is a duration of motion. This procedure determines the model parameters so as for the energy dissipation time history of the model to trace that of experiment as closely as possible. Table 4.2 shows estimated parameters. Given these parameters, equivalent damping ratios for the total system ( $h_t$ ), residual force ( $h_s$ ) and damper ( $h_d$ ) were calculated as follows.

$$h_t = \frac{c}{2\sqrt{mk}}, \quad h_s = \frac{c_s}{2\sqrt{mk}}, \quad h_d = h_t - h_s \quad (4.3)$$

Where,  $m$  is a mass of the girder. Figure 14 shows the contribution of the structural damping ( $h_s$ ) and damper ( $h_d$ ) to the total damping ratio with regard to both input motions. It is found that the supplemental dampings due to the damper increased the system's total damping almost twice as the original one. It is concluded from series of tests that the proposed damper has a capability to dissipate seismic energy effectively without transmitting excessive inertia force to the main structure even under strong motions.

Table 4.2 Identified parameters

Inputs	Stiffness (kN/m)	Damping (kN/m/sec)
Onneto	$k=3651.3$	$c=80.56$
Br.	$k_s=3170.4$	$c_s=42.64$
JR	$k=3609.6$	$c=100.75$
Takatori	$k_s=3177.2$	$c_s=51.93$

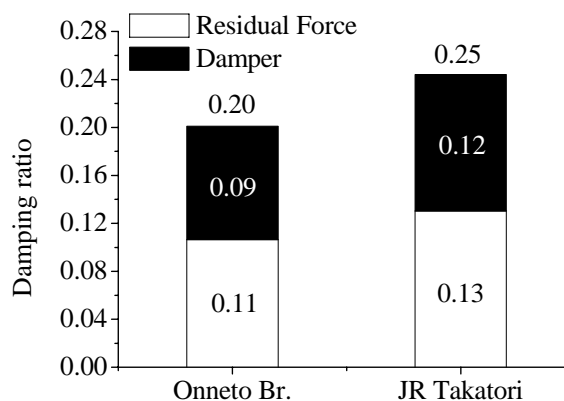


Figure 14 Estimated damping ratios due to residual force and dampers

## 5. CONCLUSION

In this research, the new friction damper applicable for civil engineering structures was newly developed. The damper holds several features advantageous over traditional structural control devices, such as tiny space for installation and easiness of performance adjustment. The prototype of the damper was assembled, and its dynamic behavior was investigated through large-scale shaking table tests. It was clearly confirmed from periodical loading tests that the device generated the stable energy dissipation and friction force regardless of the input frequency or amplitude. It was also found that the damper successfully introduced the supplemental damping to the structure under both long-term and intense earthquakes, the amount of which was approximately 10%.

## ACKNOWLEDGEMENT

The dedication of Mr. Ichikawa (Engineering staff of Kyoto University), DAMPTECH Co., Kawaguchi Metal Industries Co., Ltd., Mr. Yokita (alumnus of Kyoto Univ., now Kyushu Electric Power Company), Mr. Takahashi (graduate student of Kyoto Univ.), Nomura Jyuuki Ltd., staff and students of structural dynamics laboratory of Kyoto University for carrying out the shaking table tests is fully appreciated.

## REFERENCES

- Mualla, I.H. (2000a). Experimental Evaluation of a New Friction Damper Device, 12<sup>th</sup> World Conference on Earthquake Engineering, Auckland, New Zealand.
- Mualla, I.H. (2000b). Parameters Influencing the Behavior of a New Friction Damper Device. SPIE's 7<sup>th</sup> International Symposium on Smart Structures & Materials, SS2000, CA, USA, 2000.
- Mualla, I.H., and B. Belev. (2001) Performance of Steel Frames with a New Friction Damper Device Under Earthquake Excitation. *J. of Engineering Structures*, Elsevier (in press).
- Aiken, I.D. & Kelly, J.M. (1990). *Earthquake simulator testing and analytical studies of two energy-absorbing systems for multistory structures*. Report No. UCB/EERC-90-03, University of California, Berkeley.
- Kelly, J.M. (1999). The role of damping in seismic isolation. *Earthquake Engng. Struct. Dyn* 28:3-20.
- I. H. Mualla, L.O. Nielsen, B. Belev, W. I. Liao, C. H. Loh, A. Agrawal. (2002). Performance of Friction-Damped frame Structure: Shaking Table Testing and Numerical Simulations, 7th U.S. National Conference on Earthquake Engineering, Boston, USA.
- Nielsen LO, Mualla IH. (2004). Seismic Isolation with a Friction Damping System for Asymmetric Structures, 4th European Workshop on the Seismic Behavior of Irregular and Complex Structures, Thessaloniki, Greece.
- Nielsen LO, Mualla IH, Iwai Y. (2004). Seismic Isolation with a new Friction-Viscoelastic Damping System, 13th World Conference on Earthquake Engineering, Vancouver, Canada.
- Chopra, A K. (ed.) (1995). *Dynamics of Structures*, Prentice-Hall.